

Surface Processing of Stainless Steel Using the Channel Spark Device

M.A.I. Elgarhy^{1*}, S. Hasaballah¹, U. Rashed¹, M. El-Sabbagh¹, H. Soliman² and A. Saady¹

¹. Physics Department, Faculty of Science, Al-Azhar University, Cairo, Egypt

². Plasma and Nuclear Fusion Department, Atomic Energy Authority, Enshas, Egypt

*elgarhy@azhar.edu.eg

Abstract: This paper represents the surface treatment of stainless steel using the electron beam generated by a channel spark device after 400 treatment shoots, The electrical measurements showed that the maximum discharge current was 500 A at 10 kV charging voltage and the beam current 400 A. The stainless steel samples were characterized using XRD, EDX, SEM and micro-hardness. XRD spectra reveal that the treatment leads to the γ_N solid solution formation. EDX spectra shows that nitrogen peak began to increase from 24.733 % for untreated sample to 86.487% in the treated sample. It was also found that the hardness is 1500 VHN on the surface of the treated sample. The surface morphology by the SEM showed that the film deposited has more overlapping semi-flat layers than columnar growth like form of the untreated sample.

[Elgarhy M, Hasaballah S, Rashed U, El-Sabbagh M, Soliman H and Saady A. **Surface Processing of Stainless Steel Using the Channel Spark Device.** *Nat Sci* 2015;13(8):127-131]. (ISSN: 1545-0740).

<http://www.sciencepub.net/nature>. 20

Keywords: Stainless steel Nitridation; Electron beam ablation; Channel spark device

1. Introduction

Steel nitridation is conventionally used in surface treatment to improve surface hardness, wear [1], fatigue [2] and corrosion resistance [3]. Because the nitrogen diffusion coefficient in steel is very small at low temperature, gaseous nitridation is generally performed at a temperature range of 500–600 °C. Gaseous nitridation also needs a considerable long duration to ensure enough nitrogen diffusion length and the optimum nitrogen profile. The long duration and high temperature classically used for thermal gaseous nitridation are the causes of undesirable deformation and structural modifications of starting materials, with expensive costs of manufacture.

Decreasing the nitridation temperature improving the nitridation speed are always of great concerns of materials processing researchers [3] [4].

There are several well-known nitriding methods such as gas nitriding, plasma nitriding, laser nitriding, reactive magnetron sputtering and nitrogen implantation, and plasma immersion ion implantation [5].

Some of important advantages of plasma nitriding [6, 7] include dimensional accuracy of the surface, higher ductility of nitride layers, better mechanical properties, surface free annealing and reduction in nitriding time from about 24 hour in the conventional method to that of 3-5 hours in the ion-nitriding process [8, 9].

On the other hand pulsed electron-beam ablation has been increasingly employed for the growth of thin films [10] of simple and multicomponent materials with a wide range of

properties. Different applications (for instance, surface treatment, electron beam welding, target ablation, and gas decontamination) of the electron beams determine specific requirements for the operation parameters (current amplitude, duration, and background gas pressure) of the plasma electron beam sources [11]. A comparative study of the intense electron beams generated in the transient hollow cathode discharges [12] revealed that one of the most appropriate pulsed electron beam for material ablation is that produced in the channel spark discharge. The channel spark device is a pseudo-spark-like device with the usual multiple, hollow electrodes between anode and cathode replaced by a long, continuous dielectric tube [13]. The pulsed electron beams generated in the channel spark device propagate in a self-focused way due to the space-charge neutralization, have typical parameters: currents of tens to hundreds of A, pulse widths of tens to hundreds of ns, and energies up to tens of keV [14].

In this paper we use the electron beam generated by a channel spark device for surface processing of stainless steel. The paper is organized as follows, first we introduce the experimental setup used for the generation of the electron beam which include a simple description of a homemade channel spark device. Electrical characterization of the device and application of the electron beam for steel processing are explained in details. Finally the structure and composition of processed steel at 400 shoots are presented and characterized using XRD, EDX, SEM and micro-hardness.

2. Experimental technique

Schematic diagram of the channel spark device and its electric circuit is shown in figure (1). The channel spark device consists of a transient hollow cathode connected to a dielectric acceleration tube. The dielectric tube (6 mm diameter and 100 mm length) is connected through a narrow exit to the transient hollow cathode and picks up the electron flow for the final acceleration which forms the electron beam. The inner wall of the deposition chamber is the actual anode.

At a certain voltage a spark closes the air gap switch and its resistance becomes zero. As a consequence a rapid variation of the electric field occurs in the trigger bulb. The fast electric field variation ionizes the gas molecules (or atoms) and originates plasma, providing electrons in the hollow cathode cavity, where the discharge amplification occurs.

The stainless steel surface treatment was performed by a channel spark device using a 5 cm diameter steel target. The chamber was initially evacuated to a vacuum of the order of 4×10^{-4} Torr by using a diffusion pump. The air was supplied as a reactive gas to the device, the working gas pressure was maintained at 5 mTorr. The external capacitor, connected between the hollow cathode and the grounded anode, was 18 nF, and the applied voltage was 11 kV. The distance between the target and the substrate was fixed at 0.5 cm. The electron beam current was 80 A with energy of 2 KeV these electrons have sufficient energy to cause sputtering on the target.

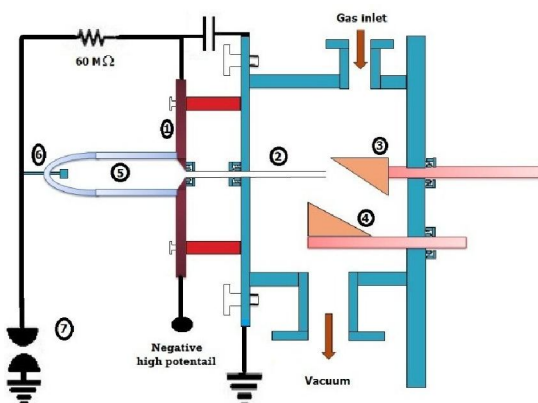


Figure 1. (a) Schematic diagram of the channel spark device and its electric circuit, 1- the hollow cathode, 2- the acceleration tube, 3- Target, 4-substrate holder, 5- the hollow cathode triggering tube, 6- trigger electrode and 7- the spark gap

The crystalline structure of the surface was analyzed by X-ray diffractometer (Panalytical Xpert

Pro, Cu-K α target 45kv 40 mA). Elemental analysis was done using EDX micro analysis (JEOL-JSM-5500LV). The surface morphology of the surface was characterized by using scanning electron microscope (JEOL-JSM-5500LV) using high vacuum mode, the samples were coated by gold sputter coater (SPI-Module). Micro-hardness measurements were made at the surface as well as along the cross section using a Vicker's hardness indenter (50 g, 20 s) (Leitz Wezzler, Germany).

3. Results and Discussion

3.1. Electron beam characteristics

The discharge current and voltage for air as a working gas was measured at different applied voltage, gas pressure and external capacitance.

Typical discharge current and voltage waveforms are shown in figure (2). This graph shows that the current reached a maximum value of 500 A after a very short period ~ 300 nsec from the beginning of the discharge. The voltage started from negative 10 kV then falls to zero after 500 nsec.

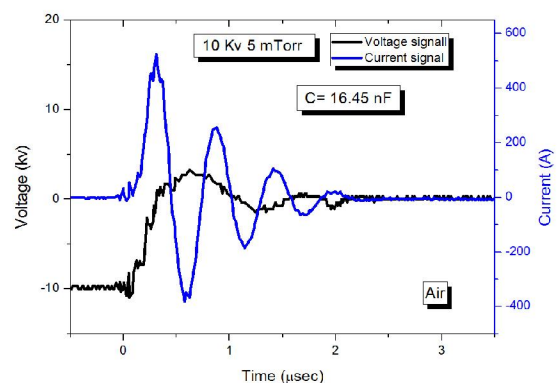


Figure 2. Discharge voltage and current waveforms at 10 kV, 5 mTorr for air gas

Figure (3) Shows the discharge current and electron beam current signals at 10 kV, 5 mTorr for air. The electron beam was measured by the Faraday cup positioned at 4 cm from the end of the tube at 10 kV, 5 mTorr for air. It was found that maximum electron beam current 80 A.

The electron beam current at different applied voltages was measured by Faraday cup located at different positions from the exit side of the dielectric tube, it was found that the electron beam current decreases with the distance from the tube end, Also it is noted that the electron beam current was increased by increasing the charging voltage as indicated in figure (4). The increase of the beam current with voltage is due to increase in the total energy injected to the system.

The decrease in the beam current with distance is mainly due to the electron scattering by gas molecules which results in the decreasing in the total number of electrons reaching to the Faraday cup.

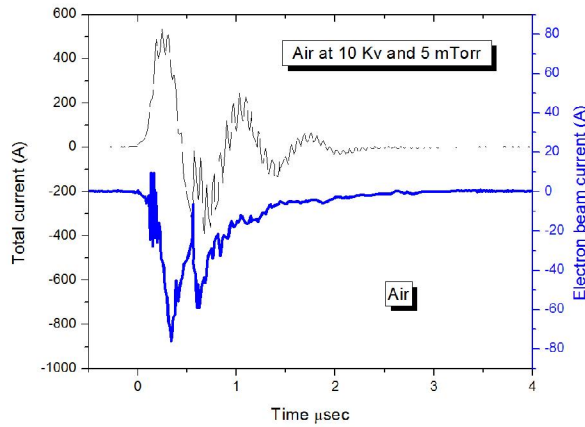


Figure 3. Discharge current and electron beam current at 10 kV, 5 mTorr for air gas

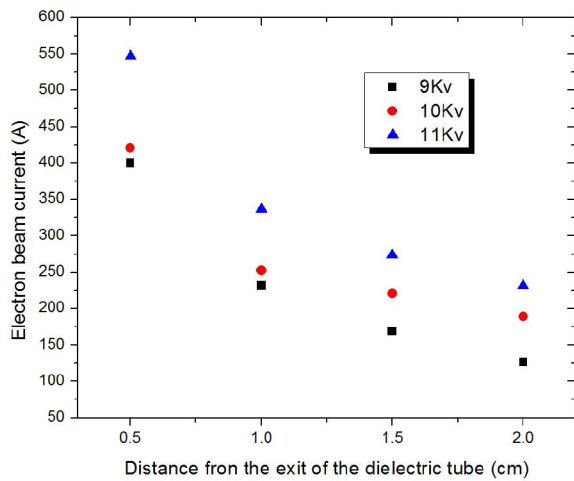


Figure 4. Variation of the electron beam current with the distance from the exit of the small dielectric tube

3.2. XRD analysis

The available grades of stainless steel can be classified into five basic families: ferritic, austenitic, duplex and precipitation hardenable.

Results of structural analysis by X-ray diffraction for the untreated and treated samples are presented in figure (5). In the untreated sample, it is noted the presence of the martensitic and the austenitic phases. In the treated sample the intensity of both of these two phases decreased in addition new phases represents the surface nitridation appeared. These new phases are mainly $\gamma_N(200)$, $\gamma_N(111)$ and

$Cr_2N(110)$. The martensitic presence is related to a mechanical polishing effect [15].

The experimental austenite lattice parameter, calculated from (2 0 0) plans, $a = 3.5948 \text{ \AA}$. It corresponds to the austenitic stainless steel AISI 304 (JCPDS 33-397) structure with a lattice parameter $a = 3.591 \text{ \AA}$.

In Fig. (5), the XRD spectrum shows also the effects of nitridation on the sample surface structure. The nitridation treatment leads to the γ_N solid solution formation. This γ_N structure can be described as a nitrogen-saturated structure without any detectable nitride formation. This is due to a preferential arrangement of the nitrogen atoms into the (2 0 0) oriented grains [16].

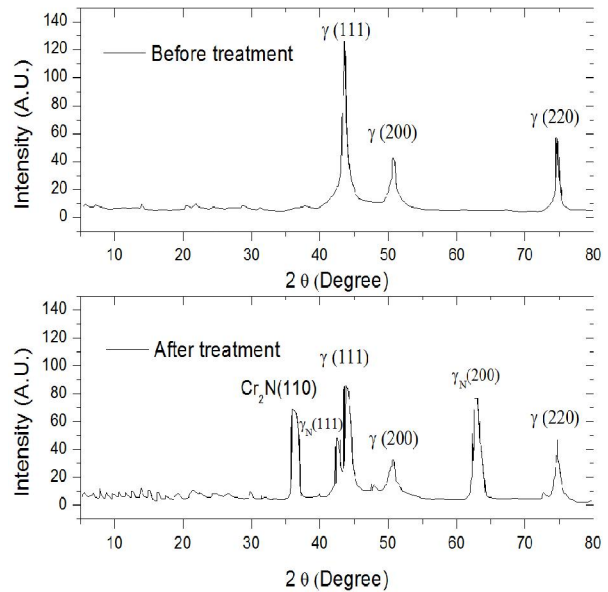


Figure 5. XRD spectrum of the Stainless steel Nitride before and after the nitridation process

The steel nitridation process in this experiment is limited to the surface only since a thin layer of CrN is formed, it acts as a diffusion barrier for further nitrogen diffusion. [17].

3.3. Energy-dispersive x-ray (EDX) analysis

Table (1) shows the EDX analysis of stainless steel sample before and after treatment.

It is clearly seen from the table that the Nitrogen content in the treated sample (86.487%) is 3.5 times more than that of the untreated sample (24.733 %).

This is due to the attachment of the nitrogen to different elements in the surface of the sample, i.e. surface nitridation, which is in good agreement with the XRD results.

Table 1. Percentage of elements in EDX spectra for treated and untreated stainless steel

Elements	Untreated stainless steel	Nitrided stainless steel
N	24.733 %	86.487%
Si	0.011 %	0.143 %
Ca	0.033 %	0.063 %
Cr	2.92 %	2.653 %
Fe	10.243 %	8.743%
Co	0.310 %	0.387 %
Ni	1.583 %	1.317 %
Cu	0.09 %	0.3 %
F	62.48 %	0 %

It is to be noted also that the fluorine content is almost vanished, this is due to cleaning of the surface by electron beam ablation (untreated sample 62.48 % and 0 % treated sample).

3.4. Micro-hardness

Figure (6) shows the variation of the surface micro-hardness at different distance from the surface of the specimen before and after treatment. It is found that the hardness drops from 1500 VHN at the surface of the specimen (treated layer) to 250 VHN at a distance of 0.1 mm far from the surface. The decreasing in hardness profile along the treated case is in accordance with the expected decrease in the nitrogen concentration as we move away from the surface.

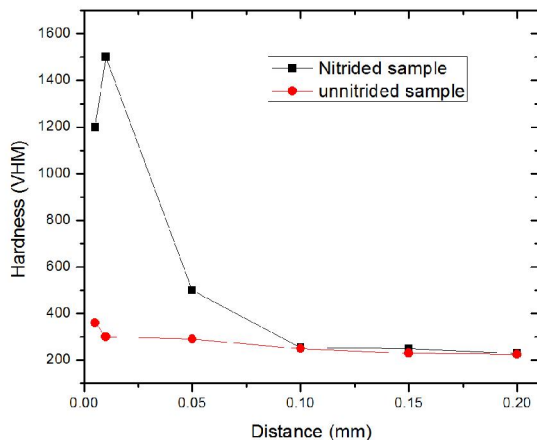


Figure 6. Cross-sectional micro-hardness profile along a specimen before and after treatment

3.5. Surface Morphology

Figure (7 a and b) shows SEM photographs of untreated and 130nitride stainless steel.

The untreated sample (Figure 7 a) is characterized by the presence of columnar layers. This columnar structure is due to the mechanical

polishing effect and the presence of the martensitic phase, as appeared in the XRD spectrum of the sample. After treatment the intensity of this phase decreased resulting in more deposited overlapping semi flat layers (Figure 7 b) than columnar growth like form of the untreated sample.

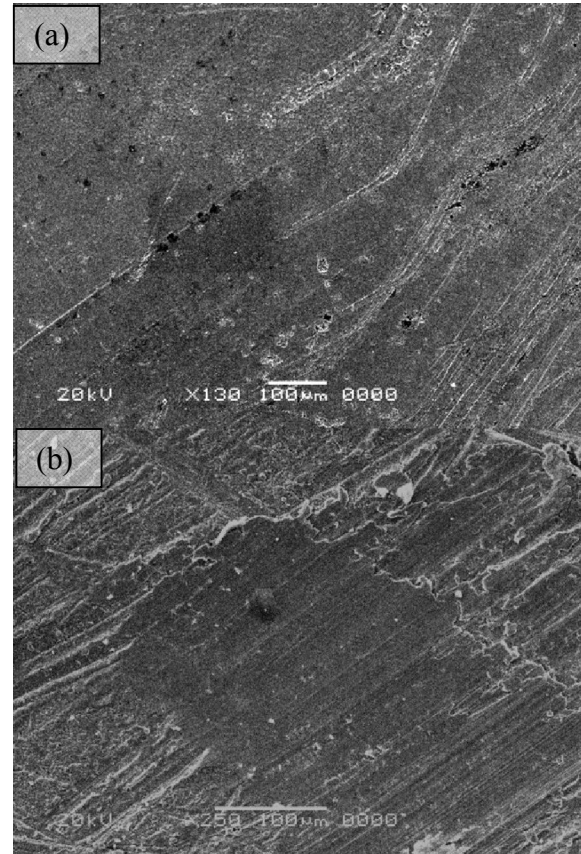


Figure 7. SEM surface scan for untreated and nitride stainless steel respectively

4. Conclusion

Nitrided stainless steel obtained by 400 deposition shoots of the channel spark device, XRD and EDX analysis reveals the formation of the nitride groups after treatment. Also Hardness increased from 250 VHN to 1500 VHN after the deposition process. SEM photographs showed the deposited layer with semi-flat structure on the surface of the sample.

Corresponding Author:

Dr. M. Elgarhy
Physics Department
Faculty of Science
Al-Azhar University, Cairo, Egypt
E-mail: elgarhy@azhar.edu.eg

References

1. M. Karamis, *Thin Solid Films*, vol. 217, p. 38, 1992.
2. T. Weber and et.al, *Mater. Sci. Eng.*, vol. A 199, p. 205, 1995.
3. L. Marot, L. Pichon, M. Drouet and A. Straboni, *Mater. Lett.*, vol. 44, p. 35, 2000.
4. K. Nishimaki, *Nanostruct. Mater.*, vol. 12, p. 527, 1999.
5. P. Schaaf, *Prog. Mater. Sci.*, vol. 47, p. 1, 2002.
6. CK. Jones and Sw.Martin, *Met Prog*, vol. 85, p. 95, 1964.
7. J. PC, *J Vac Sci Technol*, vol. 15, p. 313, 1978.
8. Lebrun JP, Michel H and Gantois M, *Mem Sci Rev Metall*, vol. 69, p. 727, 1972.
9. Michel H, Czerwiec T, Gantois M and Ablitzer DR., *Surf. Coating Technol*, vol. 103, p. 103, 1995.
10. Y. F. Ivanov, *Steel in Translation*, vol. 44, p. 573, 2014.
11. Welford and Matthew F., *Phys. Chem. Chem. Phys.*, vol. 15, p. 4422, 2013.
12. K. Frank, E. Dewald, C. Bickes, U. Ernst and M. Iberl, *IEEE Trans. Plasma Sci.*, vol. 27, p. 1008, 1999.
13. Schultheiss and G. Muller, in *Proceedings of 10th International Conference On High Power Particle Beams*, San Diego, 1994.
14. Muller G, Konijnenberg M, Krafft G and Schultheiss, vol. 89, Singapore, 1995.
15. C. Issartel, H. Buscail, E. Caudron and et. all, *Corrosion Science*, vol. 46, p. 2191, 2004.
16. C. Blawert, B.L. Mordike, Y. Jiraskova and O. Scheewe, *Surf. Eng.*, vol. 16, p. 469, 1999.
17. W. Mayr, W. Lengauer, P. Etmayer and D. Rafaja, *J. Phase. Equilib*, vol. 20, p. 35, 1999.

8/3/2015